Supporting information† for

Creating larger pores and higher stability of MOF for gas separation through continuous structure transformation

Lin Zhang[1], Gang-Ding Wang[1], Bin Zhang[1], Guo-Ping Yang[1], Wen-Yan Zhang[1], Lei Hou[1]*, Yao-Yu Wang[1], and Zhonghua Zhu[2]

[1] Key Laboratory of Synthetic and Natural Functional Molecule of the Ministry of Education, National Demonstration Center for Experimental Chemistry Education (Northwest University), College of Chemistry & Materials Science, Northwest University, Xi'an 710069, P. R. China [2] School of Chemical Engineering, The University of Queensland, Brisbane 4072, Australia

*Corresponding Author: lhou2009@nwu.edu.cn

Content

1. Comparison with the method of manufacturing defect/vacancy in the literature

Table S1. Comparisons between this work and similar literature.

Category	Methods	Results	Location selectivity of defect	Proving the structures by single crystal tests	Ref.
Before synthesis	Introducing missing-linker defects	Forming unsaturated metal center, but the defect concentration is limited.	No	No	*J. Am. Chem. Soc.* 2016, 138, 6636-6642
In synthesis	Perturbation-assisted synthesis	Hindering crystal growth, resulting in random defects, which will lead to partial amorphization.			*J. Am. Chem. Soc.* 2013, 135, 9572-9575
	Template-oriented synthesis	Random defects occur, and the removal of the template may cause the skeleton to collapse.			*Nat. Commun.* 2015, 6, 8847
Post synthesis	Introducing terminal ligands for substitution	Some of the original ligands fall off, forming random defects.			*ACS Cent. Sci.* 2021, 7, 1434-1440
	Introducing unstable linker	The ligands break after heating and form random defects.	Little (no position selectivity)		*Nat. Commun.* 2017, 8, 15356
	Introducing specific ligands with poor thermal stability	The specific ligands coordinate randomly and fall off after being heated to produce defects.			*J. Am. Chem. Soc.* 2018, 140, 2363-2372
	Using less stability Zn-O for hydrolysis	The ligands and metals fall off together, and one metal ion and one ligand in the cluster were removed.	Partial (no linker selectivity)		*J. Am. Chem. Soc.* 2014, 136, 14465-14471
	Introducing Cu^{2+} ions with shorter M-N bonds to replace Zn^{2+} ions	1. It becomes a more active Cu$_2$(COO)$_4$ SBU, and the adsorption performance is enhanced. 2. The Cu$_2$(COO)$_4$ paddle wheel SBU shrinks and the connecting ligand falls off. 3. The lengths of coordination bond become shorter and the stability of MOF is enhanced.	**Complete selectivity**	**Yes**	**This Work**
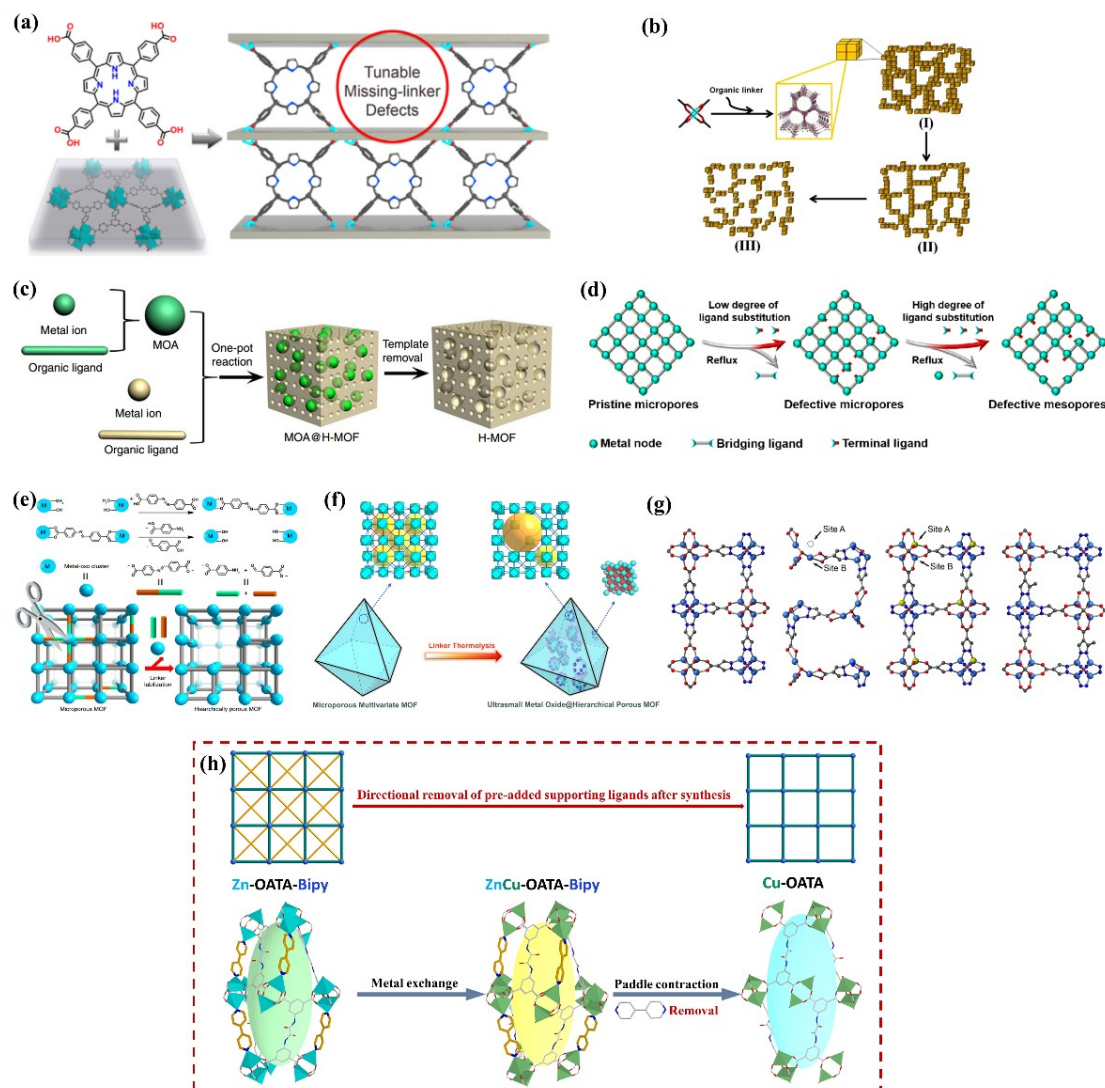
Figure S1. Schematic diagram in references (a-g) and this work (h), showing difference in methods and results.

2. Material synthesis

5,5'-(oxalylbis(azanediyl))diisophthalic acid (H$_4$OATA) was synthesized by literature methods.[1] The drugs used (5-aminoisophthalic acid, 98% and oxalyl chloride, 98%) were purchased from Energy Chemical.

(1) Synthesis of [Zn$_6$(OATA)$_3$(H$_2$O)$_4$(DMF)$_2$]·5H$_2$O·10DMF (Zn-OATA)[1]

Zn(NO$_3$)$_2$·6H$_2$O (0.12 g, 0.40 mmol) and H$_4$OATA (0.03 g, 0.07 mmol) were mixed in 6 mL of DMF at room temperature under stirring for 20 min. The solution was sealed in a glass bottle and heated at 85 °C for 24 h.

(2) Synthesis of $[Zn_6(OATA)_3Bipy_2(H_2O)_2]\cdot 4H_2O\cdot 5DMF$ **(Zn-OATA-Bipy)**

$Zn(NO_3)_2\cdot 6H_2O$ (0.0297 g, 0.10 mmol), H_4OATA (0.0412 g, 0.10 mmol), 4,4'-Bipyridine (Bipy) (0.0078 g, 0.05 mmol), N,N-Dimethylformamide (DMF, 5 mL), and concentrated HNO_3 (65%, 100 uL) was stirred and dissolved in glass bottles, heated at 105 °C for 72 h, and the yellowish block crystals of **Zn-OATA-Bipy** were obtained after cooling (yield:73%). Anal. Calcd for $C_{89}H_{87}Zn_6O_{41}N_{15}$: C, 44.30; H, 3.61; N, 8.71%. Found: C, 44.62; H, 3.48; N, 8.89%.

(3) Synthesis of $[Zn_{5.1}Cu_{0.9}(OATA)_3Bipy_2(H_2O)_2]\cdot 4H_2O\cdot 4DMF$ **(ZnCu-OATA-Bipy)**

The crystal of **Zn-OATA-Bipy** (200 mg) was immersed in the solution of 5 mL 0.5 M $Cu(NO_3)_2\cdot 2.5H_2O$ dissolved by DMF and heated at 85°C for 8-12 hours, then the bright green crystal fragments of **ZnCu-OATA-Bipy** was obtained. Anal. Calcd for $C_{86}H_{80}Cu_6O_{40}N_{14}$: C, 43.14; H, 3.34; N, 8.19%. Found: C, 43.56; H, 3.52; N, 8.03%.

(4) Synthesis of $[Cu_2(OATA)(H_2O)_2]\cdot 2H_2O\cdot 4DMF$ **(Cu-OATA)**

The crystal of **Zn-OATA-Bipy** (200 mg) was immersed in the solution of 5 mL 0.5 M $Cu(NO_3)_2\cdot 2.5H_2O$ dissolved by DMF and heated at 105°C for 24 hours, then the dark green crystal frgments of **Cu-OATA** was obtained (yield:96%). Anal. Calcd for $C_{30}H_{44}Cu_2O_{18}N_6$: C, 39.82; H, 4.87; N, 9.29%. Found: C, 44.91; H, 5.02; N, 8.19%.
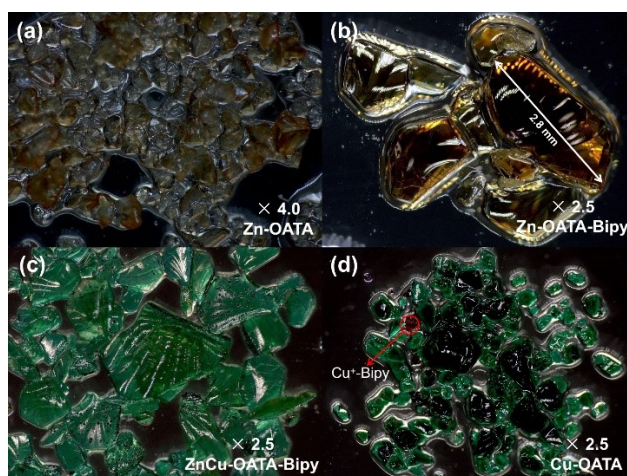
Figure S2. The crystal appearance of (a) Zn-OATA, (b) Zn-OATA-Bipy, (c) ZnCu-OATA-Bipy, and (d) Cu-OATA under the microscope.
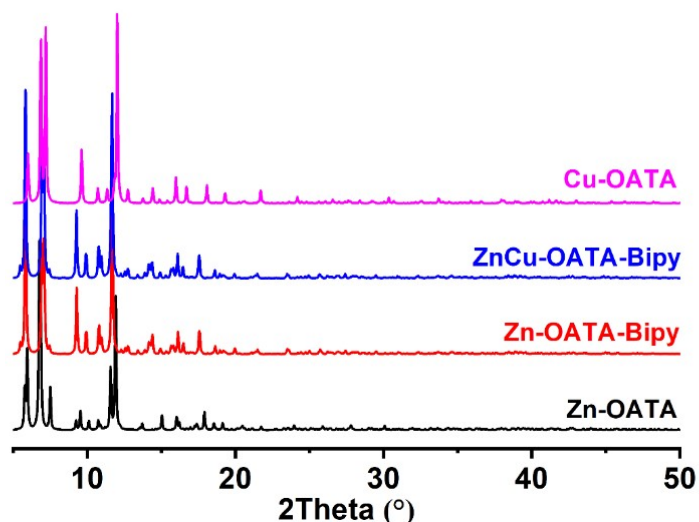
Figure S3. PXRD patterns of four MOFs.

3. Scanning electron microscope (SEM)
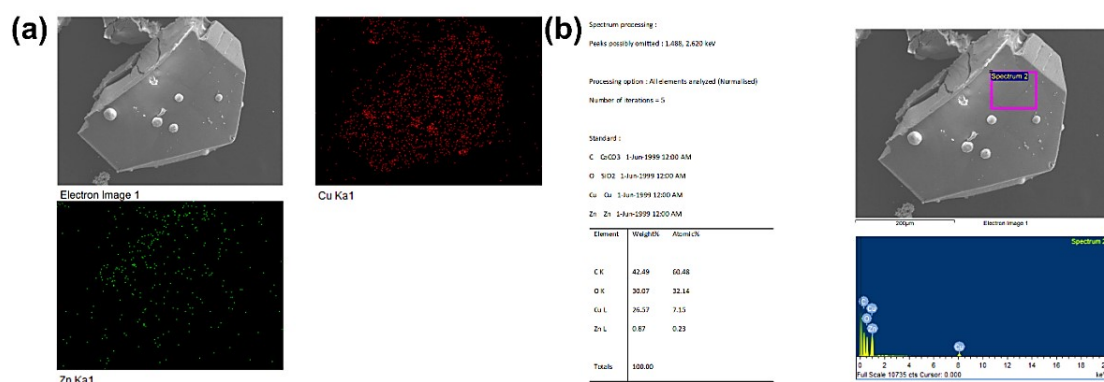
Figure S4. Mapping (a) and EDS (b) analysis of ZnCu-OATA-Bipy.

4. X-ray crystallographic measurements

The single crystal diffraction data was conducted at 200(2) K on a Bruker SMART APEX II CCD detector diffractometer. The structure was solved by direct method and refined on F^2 by full-matrix least-squares procedures with SHELXL-2014 software package. The non-hydrogen atoms were refined anisotropically, while the hydrogen atoms added to their geometrically ideal positions and were refined isotropically. For the disordered lattice molecules that cannot be well refined, the SQUEESE procedure was adopted in structural refinement. The results of structure refinement are listed in Tables S1.

Table S2. Crystallographic data of five MOFs.

	Zn-OATA[1]	Zn-OATA-Bipy	ZnCu-OATA-Bipy	Cu-OATA	Cu⁺-Bipy
Empirical formula	$C_{30}H_{23}Zn_3N_4O_{18}$	$C_{74}H_{44}Zn_6N_{10}O_{32}$	$C_{74}H_{44}Cu_{0.9}N_{10}O_{32}Zn_{5.1}$	$C_{18}H_{12}Cu_2N_2O_{12}$	$C_{11}H_9CuN_2O_2$
Formula weight	923.63	1977.41	1975.76	575.38	264.74
Crystal system	Triclinic	Monoclinic	Monoclinic	Trigonal	Orthorhombic
Space group	P-1	P2$_1$/c	P2$_1$/c	R-3m	Fddd
a (Å)	16.6706(2)	27.6797(15)	27.7020(18)	18.5090(9)	9.570(2)
b (Å)	16.6706(2)	19.0412(12)	19.0518(10)	18.5090(9)	13.1650(16)
c (Å)	17.7165(2)	32.9249(19)	33.007(2)	38.449(4)	32.976(5)
	65.501(3)	90	90	90	90
α, β, γ (°)	65.445(3)	112.962(2)	113.014(2)	90	90
	69.980(4)	90	90	120	90
Z, V (Å³)	2, 3988.2(5)	4, 15978.2(16)	4, 16033.8(17)	9, 11407.3(16)	16, 4154.7(12)
D_c (g cm⁻³), μ (mm⁻¹)	0.769, 0.93	0.822, 0.933	0.818, 0.915	0.475, 4.710	1.693, 2.086
R_{int}, GOF	0.263, 1.086	0.1190, 1.077	0.0519, 1.051	0.2138, 1.150	0.0882, 1.135
R_1[a], wR_2[b] [I > 2σ]	0.173, 0.507	0.0866, 0.2712	0.0380, 0.1172	0.2667, 0.2352	0.0788, 0.2374

[a]$R_1 = \Sigma||F_o| - |F_c||)/\Sigma|F_o|$; [b]$wR_2 = [\Sigma w(F_o^2 - F_c^2)^2/\Sigma w(F_o^2)^2]^{1/2}$.

Figure S5. Coordination structure diagram of Cu⁺-complex [Cu(Bipy)](HCOO).

Figure S6. (a) and (b) 3D porous framework of Zn-OATA-Bipy; (c) and (d) 3D porous framework of Cu-OATA.

5. Powder X-ray diffraction (PXRD) and thermogravimetric analysis (TGA)

Figure S7. PXRD patterns of Zn-OATA-Bipy (a) and Cu-OATA (b) after different treatments.

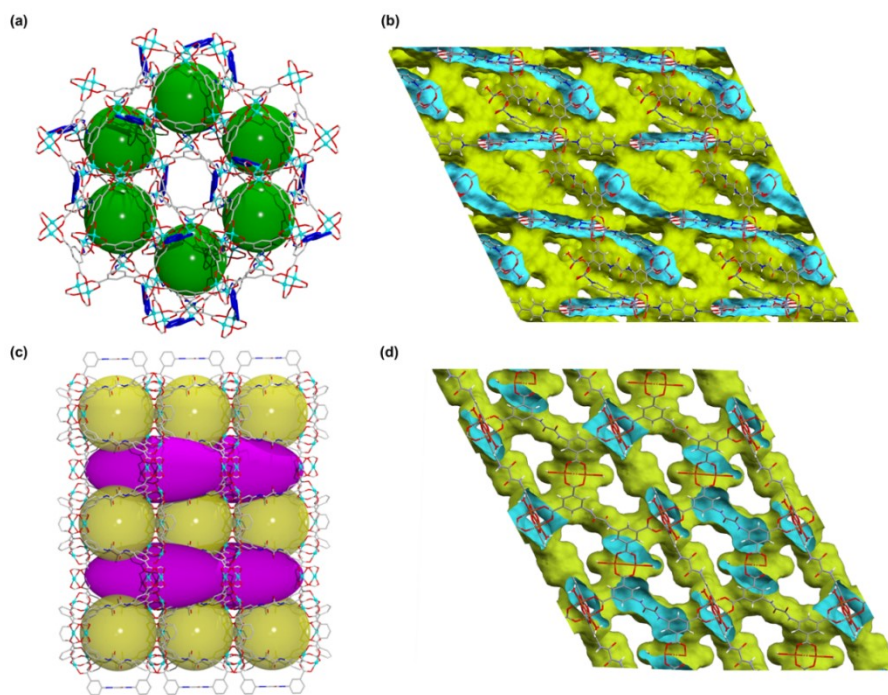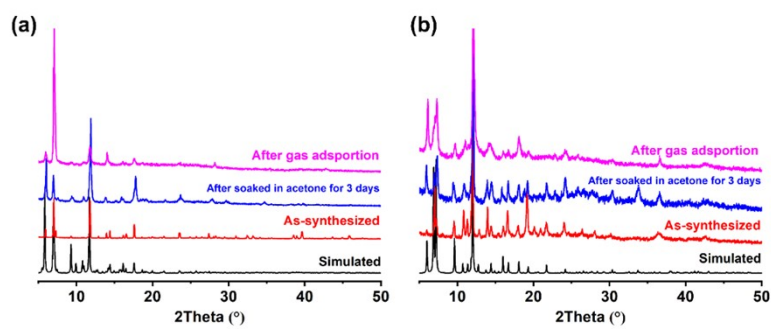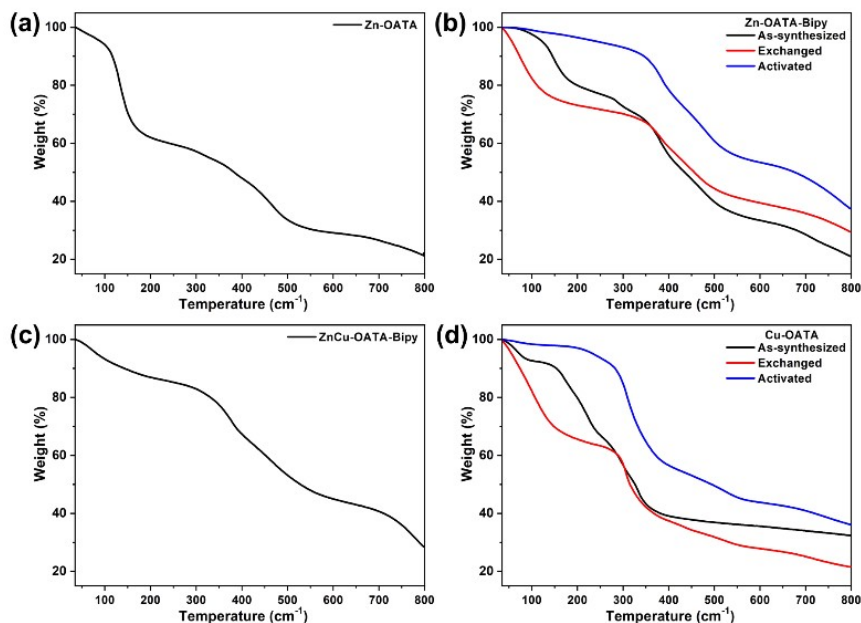**Figure S8.** TGA curves for (a) Zn-OATA, (b) Zn-OATA-Bipy, (c) ZnCu-OATA-Bipy, and (d) Cu-OATA.

6. Calculation of sorption heat using Virial 2 model

$$\ln P = \ln N + 1/T \sum_{i=0}^{m} a_i N^i + \sum_{i=0}^{n} b_i N^i \qquad\qquad Q_{st} = -R \sum_{i=0}^{m} a_i N^i$$

The above virial expression was used to fit the combined isotherm data (measured at 273 and 298 K), where P is the pressure, N is the adsorbed amount, T is the temperature, a_i and b_i are virial coefficients, and m and N are the number of coefficients used to describe the isotherms. Q_{st} is the coverage-dependent enthalpy of adsorption and R is the universal gas constant.

Table S3. Fitting parameters of the adsorption heats for Zn-OATA-Bipy.

	C_3H_6	C_2H_4	C_3H_8	C_2H_6	CH_4
a0	-4493.31818	-3428.69342	-4269.6955	-3409.58636	-2252.24369
a1	-19.35683	-7.30804	-19.68291	-9.63865	-3.03345
a2	-0.0053	0.22919	0.00473	0.34768	27.86805
a3	8.27951E-5	-0.00333	8.98611E-5	-0.00412	-3.05959
a4	3.6995E-8	1.677E-5	3.00345E-8	1.67157E-5	0.11049
b0	13.89103	13.50398	13.38634	13.09105	12.38592
b1	0.06958	0.01571	0.06549	0.00491	-0.30351
R^2	0.99857	0.99867	0.99916	0.99032	0.99629
Chi^2	0.00504	0.00421	0.00404	0.03042	0.00969

7

Table S4. Fitting parameters of the adsorption heats for Cu-OATA.

	C_3H_6	C_2H_4	C_3H_8	C_2H_6	CH_4
a0	-4622.94516	-4049.93224	-4581.80228	-3939.11189	-2406.76031
a1	-11.48153	8.00776	-11.97857	14.60514	12.30092
a2	-0.02917	-0.1051	-0.03087	-0.03855	0.79196
a3	6.71355E-5	7.04471E-4	1.19417E-4	1.48593E-4	-0.0777
a4	-9.7087E-9	-1.63657E-6	-7.58029E-8	1.78643E-7	0.00224
b0	12.80082	13.59438	14.41469	14.58559	12.37599
b1	0.0617	0.00818	0.05016	-0.03588	-0.0382
R^2	0.99787	0.99997	0.99819	0.99967	0.99996
Chi^2	0.00504	0.00421	0.00404	0.03042	0.00969
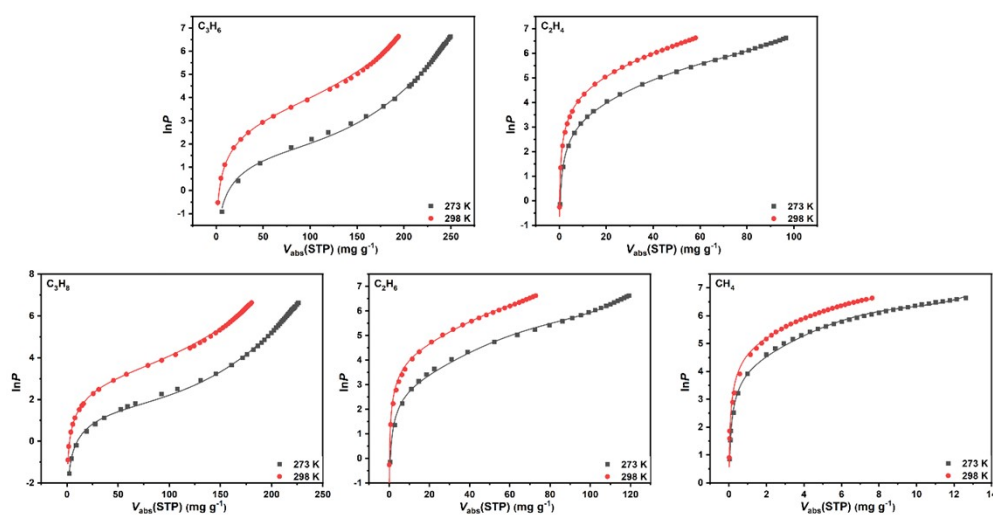
Figure S9. Adsorption isotherms of Zn-OATA-Bipy fitted by Virial 2 model.
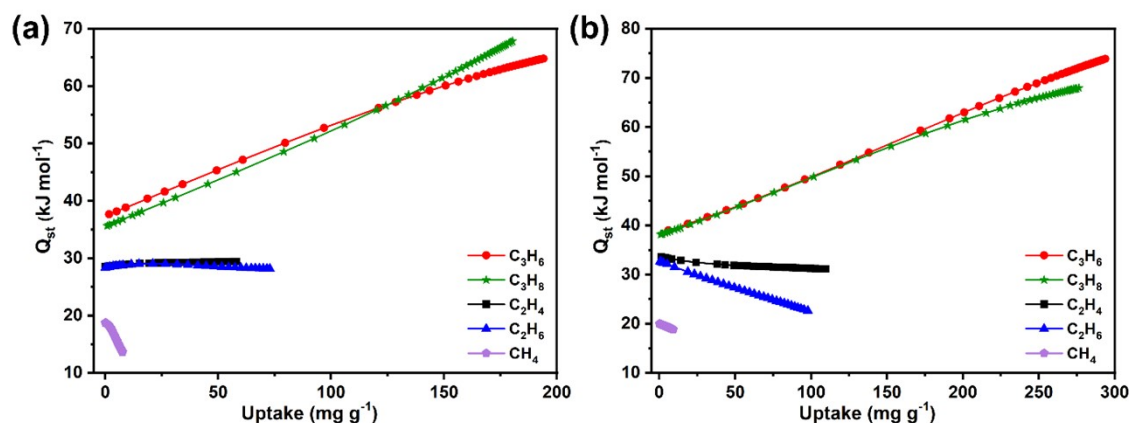
Figure S11. Adsorption heats of the gases.

7. IAST adsorption selectivity calculation

The experimental isotherm data for pure gases (measured at 273 and 298 K) was fitted using a single Langmuir-Freundlich (L-F) model:

$$q = \frac{a_1 * b_1 * P^{c_1}}{1 + b_1 * P^{c_1}}$$

Where q and p are the adsorbed amounts and the pressure of component i, respectively.

The adsorption selectivity for binary mixtures defined by

$$S_{i/j} = \frac{x_i * y_j}{x_j * y_i}$$

was calculated using the Ideal Adsorption Solution Theory (IAST) of Myers and Prausnitz. Where x_i is the mole fraction of component i in the adsorbed phase and y_i is the mole fraction of component i in the bulk.

Table S5. Fitting parameters of C_3H_6/C_2H_4 selectivity for Zn-OATA-Bipy at 273/298 K.

	273 K		298 K	
	C_3H_6	C_2H_4	C_3H_6	C_2H_4
A1	5.98352	5.05629	4.88851	4.17689
b1	0.55577	0.02246	0.12717	0.00977
c1	0.87673	0.9916	1.02103	1.00182
R^2	0.99676	0.99996	0.99966	1

	Chi^2	0.00829	5.61741E-5	7.89241E-4	1.63424E-6

Table S6. Fitting parameters of C_3H_6/C_2H_4 selectivity for Cu-OATA at 273/298 K.

	273 K		298 K	
	C_3H_6	C_2H_4	C_3H_6	C_2H_4
A1	9.38215	8.8593	7.93612	7.83922
b1	0.49889	0.06689	0.15652	0.02939
c1	0.82047	0.71295	0.84039	0.76249
R^2	0.99862	0.99997	0.99889	0.99998
Chi^2	0.00795	1.26301E-4	0.00573	3.15536E-5

Table S7. Fitting parameters of $C_3H_8/C_2H_6/CH_4$ selectivity for Zn-OATA-Bipy at 273/298 K.

	273 K			298 K		
	C_3H_8	C_2H_6	CH_4	C_3H_8	C_2H_6	CH_4
A1	5.12575	3.71688	6.5668	4.27171	3.37411	3.01235
b1	0.51453	0.03205	0.00165	0.12908	0.01251	0.00186
c1	0.9281	1.04757	0.95886	1.04931	1.02965	0.99827
R^2	0.99687	0.99991	0.99995	0.9993	0.99996	0.99994
Chi^2	0.00909	1.05484E-4	3.15843E-6	0.00157	2.1342E-5	1.38876E-6

Table S8. Fitting parameters of $C_3H_8/C_2H_6/CH_4$ selectivity for Cu-OATA at 273/298 K.

	273 K			298 K		
	C_3H_8	C_2H_6	CH_4	C_3H_8	C_2H_6	CH_4
A1	7.89815	7.63679	7.49583	6.44607	8.2071	7.93184
b1	0.3041	0.01994	0.00189	0.04575	0.00278	8.67894E-4
c1	1.28579	1.05782	0.96799	1.36972	1.18733	0.97628
R^2	0.99695	0.99932	1	0.99932	0.99981	0.99999
Chi^2	0.02555	0.0022	3.1822E-7	0.00421	2.33474E-4	2.22759E-7

Figure S12. C$_3$H$_6$ and C$_2$H$_4$ adsorption isotherms fitting for Zn-OATA-Bipy at 273/298 K.
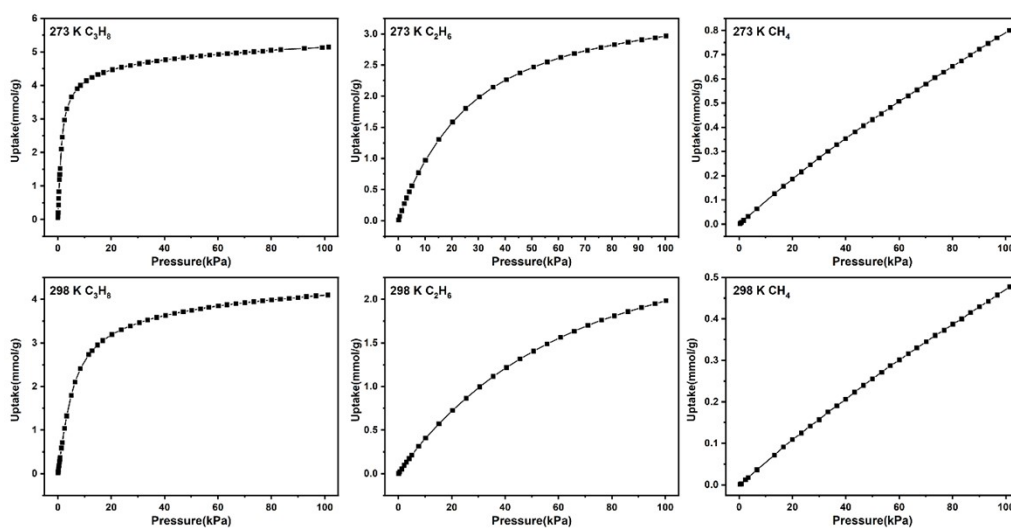
Figure S13. C$_3$H$_8$, C$_2$H$_6$ and CH$_4$ adsorption isotherms fitting for Zn-OATA-Bipy at 273/298 K.

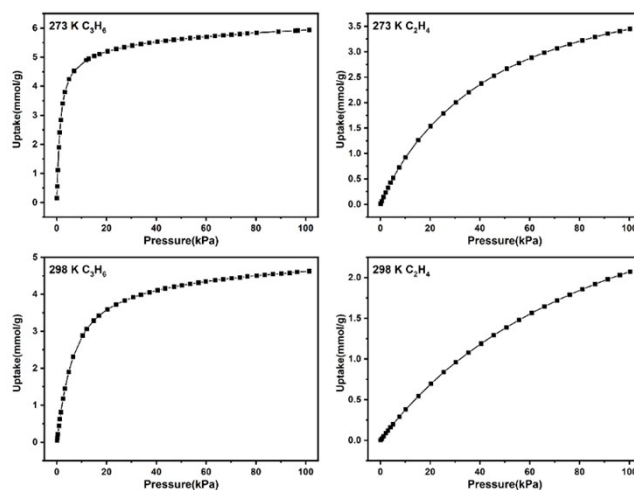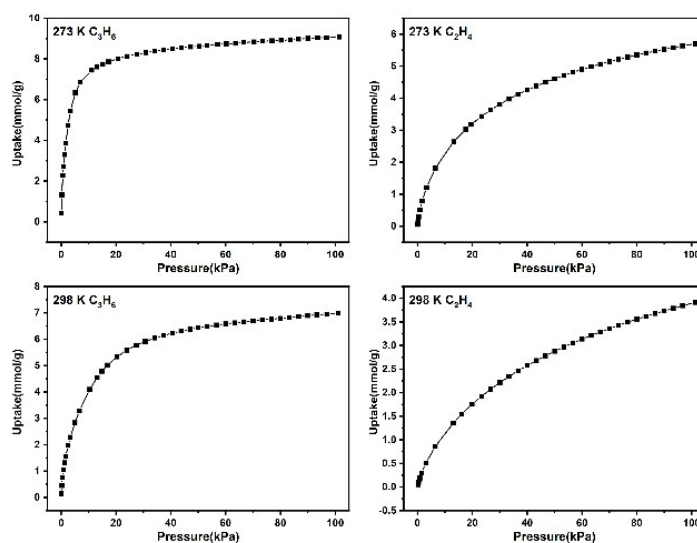**Figure S14.** C_3H_6 and C_2H_4 adsorption isotherms fitting for Cu-OATA at 273/298 K.
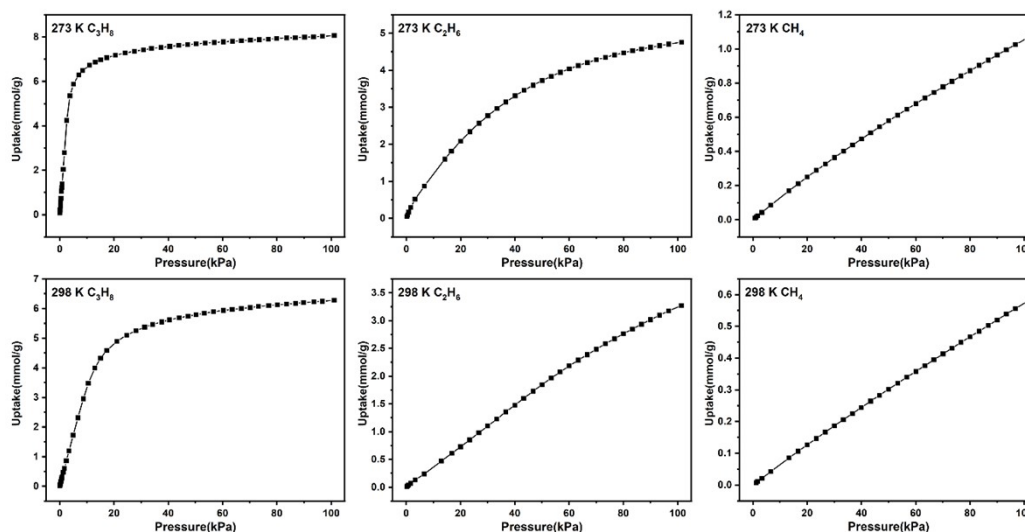
Figure S15. C_3H_8, C_2H_6 and CH_4 adsorption isotherms fitting for Cu-OATA at 273/298 K.

Table S9. Adsorption capacity and selectivity of C_3H_6/C_2H_4 at 1 atm and 298 K for the molar ratio at 50:50 binary mixtures of the promising MOFs

	C_3H_6 Uptake (cm^3 g^{-1})	C_2H_4 Uptake (cm^3 g^{-1})	IAST Selectivity	Ref.
Zn-OATA-Bipy	**113.3**	**50.8**	**19.8**	**This work**
Cu-OATA	**171.4**	**95.9**	**10.8**	**This work**
LIFM-WZ-3	44	32	10.7	2
ANPC-2-700	203.4	105.1	9.8	3
NEM-7-Cu	75.5	29	8.6	4
MFM-202a	160.8	64.96	8.4	5
spe-MOF	236.9	21.4	7.7	6
iso-MOF-4	254.5	73.1	7.7	7
NEM-4	197.4	164.1	6.8	8
HKUST-1	137.4	102.14	5.8	9
UPC-33	94.3	31.1	5.7	10
iso-MOF-1	209	71.4	5.1	7
(Cr)-MIL-101-SO$_3$Ag	105.84	63.95	4.8	11
Zn-BPZ-SA	68.3	63.9	4.8	12
Mg-MOF-74	149.98	161.28	4.7	13
PCP-1	70.7	56.67	3.6	14

Table S10. Adsorption capacity and selectivity of C_3H_8/C_2H_6/CH_4 at 1 atm and 298 K for the molar ratio at 50:50 binary mixtures of the promising MOFs

	C_3H_8 Uptake (cm^3 g^{-1})	C_2H_6 Uptake (cm^3 g^{-1})	CH_4 Uptake (cm^3 g^{-1})	C_3H_8/C_2H_6 Selectivity	C_3H_8/CH_4 Selectivity	C_2H_6/CH_4 Selectivity	Ref.
SNNU-Bai68	77	69	23.4	9.2	232.3	22.4	15
SNNU-Bai69	55	43	7	6.8	214.4	25.3	16
Zn-OATA-Bipy	**100.4**	**48.6**	**11.7**	**18.4**	**195.7**	**8.5**	**This work**
CTGU-15	297.2	52.2	9.8	5.2	170.2	5.2	17
NEM-4	196.1	172.2	19.3	6.2	168.3	20.1	8
MOF-801	74	55.4	12.8	11.8	136.8	22	18
UPC-98	97.4	45.4	5.9	5.9	124.6	13.6	19
A-AC-4	288.1	161.4	28.9	5.1	108.4	15.6	20
In/Tb-CBDA	61	50	8	6.7	105	12	21
UPC-35	111.3	40.9	4.8	5.6	97.7	11.6	22
InOF-1	104.1	101.4	17.2	4.9	90	17	23
A-AC-3	277.8	173.7	33.8	4.3	89.5	16.7	20
Cu-OATA	**153.9**	**80.1**	**14.2**	**9.1**	**82.8**	**8.4**	**This work**
UPC-104	232.8	133.8	18.1	5.0	79	12.3	24

8. Grand canonical Monte Carlo (GCMC) simulations

Grand canonical Monte Carlo (GCMC) simulations were performed for the gas adsorption in the framework by the Sorption module of Material Studio (Accelrys. Materials Studio Getting Started). The partial charges for atoms of the framework were derived from QEq method and QEq neutral 1.0 parameter. One unit cell was used during the simulations. The interaction energies between the gas molecules and framework were computed through the Coulomb and Lennard-Jones 6-12 (LJ) potentials. All parameters for the atoms were modeled with the universal force field (UFF) embedded in the MS modeling package. A cutoff distance of 12.5 Å was used for LJ interactions, and the Coulombic interactions were calculated by using Ewald summation. For each run, the 3×10^6 maximum loading steps, 3×10^6 production steps were employed.

9. Breakthrough experiments

The breakthrough experiment was performed on the Quantachrome dynaSorb BT equipment at 298 K and 1 atm (Ar as the carrier gas). The activated Zn-OATA-Bipy/Cu-OATA was filled into a packed column of ϕ 4.2×80 mm, and then the

packed column was washed with Ar at 343 K for 60 minutes to further activate the samples. Between two breakthrough experiments, the adsorbent was regenerated by Ar flow of 8 mL min^{-1} for 35 min at 353 K to guarantee a complete removal of the adsorbed gases.

Table S11. Breakthrough experiment for olefin at different test conditions.

C_3H_6/C_2H_4 (v/v)	Flow rate (mL min^{-1})	C_2H_4 Retention time (min g^{-1})	C_3H_6 Retention time (min g^{-1})	Δt (min g^{-1})	C_2H_4 Collection volume (cm^3 g^{-1})	C_3H_6 Collection volume (cm^3 g^{-1})	C_2H_4 Purity ($\geq$ %)	C_3H_6 Purity ($\geq$ %)
Zn-OATA-Bipy								
20/20	8	1.2	20.3	19.1	32.7	-	99.5	-
10/30	8	1.7	32.8	31.1	48.6	25.5	99.9	92
Cu-OATA								
20/20	8	13.2	47.6	33.4	87.1	-	99.9	-
10/30	8	13.5	71.8	58.3	168.4	50.3	99.95	97

Table S12. Breakthrough of some benchmark materials for olefin at 298 K.

	Flow rate (mL min^{-1})	Mixture composition and proportion (v/v)	C_3H_6/C_2H_4 Approximate retention time difference (min g^{-1})	Ref.
Cu-OATA	**8**	**$C_2H_4/C_3H_6/Ar$ = 20/20/60**	**33.4**	**This**
	8	**$C_2H_4/C_3H_6/Ar$ = 30/10/60**	**58.3**	**work**
iso-MOF-4	2.67	C_2H_4/C_3H_6 = 50/50	95	7
spe-MOF	2	C_2H_4/C_3H_6 = 50/50	67	6
	4	C_2H_4/C_3H_6 = 50/20	37	
[Zn$_2$(oba)$_2$(dmimpym)]	6	$C_2H_4/C_3H_6/Ar$ = 5/5/90	120	25
	6	$C_2H_4/C_3H_6/Ar$ = 5/2/93	165	
CR-COF-2	1	C_2H_4/C_3H_6 = 50/50	35	26
	2	C_2H_4/C_3H_6 = 50/20	37	
Mn-dtzip	8	$C_2H_4/C_3H_6/Ar$ = 20/20/60	12	27
	7	$C_2H_4/C_3H_6/Ar$ = 25/10/65	25	
Zn-OATA-Bipy	**8**	**$C_2H_4/C_3H_6/Ar$ = 20/20/60**	**19.1**	**This**
	8	**$C_2H_4/C_3H_6/Ar$ = 30/10/60**	**31.1**	**work**
Zn-BPZ-SA	5	$C_2H_4/C_3H_6/Ar$ = 5/5/90	124	12
	5	$C_2H_4/C_3H_6/Ar$ = 5/2/93	153	

Table S13. Breakthrough experiment for paraffin at different test conditions.

$C_3H_8/C_2H_6/CH_4$ (v/v/v)	Flow rate (mL min^{-1})	Δt C_3H_8-C_2H_6 (min g^{-1})	Δt C_3H_8-CH_4 (min g^{-1})	Δt C_2H_6-CH_4 (min g^{-1})	CH_4 Collection volume (cm^3 g^{-1})	C_2H_6 Collection volume (cm^3 g^{-1})	C_3H_8 Collection volume (cm^3 g^{-1})
Zn-OATA-Bipy							
20/20/0	8	11.9	-	-	-	18.3	-
0/4/34	13	-	-	1.8	6.2	-	-
2/4/34	13	21.8	24.1	2.3	8.5	-	9.1
Cu-OATA							
20/20/0	8	32.2	-	-	-	68.2	61.3
0/4/34	13	-	-	6.8	31.9	-	-
2/4/34	13	49.2	56.1	6.9	32.3	-	13.3

Table S14. Breakthrough of some benchmark materials for $C_3H_8/C_2H_6/CH_4$ = 5/10/85.

	Flow rate (mL min^{-1})	Δt C_3H_8-C_2H_6 (min g^{-1})	Δt C_3H_8-CH_4 (min g^{-1})	Δt C_2H_6-CH_4 (min g^{-1})	C_3H_8 Approximate Collection volume (cm^3 g^{-1})	CH_4 Approximate Collection volume (cm^3 g^{-1})	Ref.
Ni(HBTC)(Bipy)	5	56	76	20	-	85	28
BSF-2	4	52	67	15	-	51	29
Cu-OATA	**13**	**49.2**	**56.1**	**6.9**	**13.3**	**32.3**	**This work**
LIFM-ZZ-1	3	42	63	21	-	53.6	30
BSF-3	10	37	58	21	-	178.5	31
SNNU-Bai69	10	25.3	35.5	10.2	-	86.7	16
SNNU-Bai68	10	24	35	11	-	93.5	15
MOF-801	10	22	27.2	5.2	-	44.2	18
Zn-OATA-Bipy	**13**	**21.8**	**24.1**	**2.3**	**9.1**	**8.5**	**This work**
A-AC-3	10	19.5	33	13.5	-	114.8	20
MIL-142A	10	10	12	2	-	17	32

10. References

[1] Y. Guclu, H. Erer, H. Demiral, C. Altintas, S. Keskin, N. Tumanov, B. L. Su, F. Semerci, *ACS Appl. Mater. Interfaces* 2021, **13**, 33188-33198.

[2] Z. Wang, J.-H. Zhang, J.-J. Jiang, H.-P. Wang, Z.-W. Wei, X. Zhu, M. Pan, C.-Y. Su, *J. Mater. Chem. A* 2018, **6**, 17698-17705.

[3] P. Zhang, X. Wen, L. Wang, Y. Zhong, Y. Su, Y. Zhang, J. Wang, J. Yang, Z. Zeng, S. Deng, *Chem. Eng. J.* 2020, **381**, 122731.

[4]   X. Liu, C. Hao, J. Li, Y. Wang, Y. Hou, X. Li, L. Zhao, H. Zhu, W. Guo, *Inorg. Chem. Front.* 2018, **5**, 2898-2905.

[5]   S. Gao, C. G. Morris, Z. Lu, Y. Yan, H. G. W. Godfrey, C. Murray, C. C. Tang, K. M. Thomas, S. Yang, M. Schröder, *Chem. Mater.* 2016, **28**, 2331-2340.

[6]   H. Fang, B. Zheng, Z. H. Zhang, H. X. Li, D. X. Xue, J. Bai, *Angew. Chem. Int. Ed.* 2021, **60**, 16521-16528.

[7]   W. Fan, X. Wang, X. Zhang, X. Liu, Y. Wang, Z. Kang, F. Dai, B. Xu, R. Wang, D. Sun, *ACS Cent. Sci.* 2019, **5**, 1261-1268.

[8]   X. Liu, W. Fan, M. Zhang, G. Li, H. Liu, D. Sun, L. Zhao, H. Zhu, W. Guo, *Mater. Chem. Front.* 2018, **2**, 1146-1154.

[9]   W. Su, A. Zhang, Y. Sun, M. Ran, X. *J.* Wang, *Chem. Eng. Data* 2016, **62**, 417-421.

[10] W. Fan, Y. Wang, Q. Zhang, A. Kirchon, Z. Xiao, L. Zhang, F. Dai, R. Wang, D. Sun, *Chem. Eur. J.* 2018, **24**, 2137-2143.

[11] G. Chang, M. Huang, Y. Su, H. Xing, B. Su, Z. Zhang, Q. Yang, Y. Yang, Q. Ren, Z. Bao, B. Chen, *Chem. Commun.* 2015, **51**, 2859-2862.

[12] G.-D. Wang, R. Krishna, Y.-Z. Li, Y.-Y. Ma, L. Hou, Y.-Y. Wang, *ACS Materials Lett.* 2023, **5**, 1091-1099.

[13] X. Wu, Z. Bao, B. Yuan, J. Wang, Y. Sun, H. Luo, S. Deng, *Micropor. Mesopor. Mat.* 2013, **180**, 114-122.

[14] D. Geng, M. Zhang, X. Hang, W. Xie, Y. Qin, Q. Li, Y. Bi, Z. Zheng, *Dalton Trans.* 2018, **47**, 9008-9013.

[15] H. Cheng, Q. Wang, L. Meng, P. Sheng, Z. Zhang, M. Ding, Y. Gao, J. Bai, *ACS Appl Mater Interfaces* 2021, **13**, 40713-40723.

[16] M. Ding, Q. Wang, H. Cheng, J. Bai, *CrystEngComm* 2022, **24**, 2388-2392.

[17] D. Lv, Z. Liu, F. Xu, H. Wu, W. Yuan, J. Yan, H. Xi, X. Chen, Q. Xia, *Sep. Purif. Technol.* 2021, **266**, 118198.

[18] H. Liu, B. Li, Y. Zhao, C. Kong, C. Zhou, Y. Lin, Z. Tian, L. Chen, *Chem. Commun.* 2021, **57**, 13008-13011.

[19] X. Wang, X. Wang, X. Zhang, W. Fan, Q. Li, W. Jiang, F. Dai, D. Sun, *Cryst. Growth Des.* 2020, **20**, 5670-5675.

[20] W. Liang, H. Xiao, D. Lv, J. Xiao, Z. Li, *Sep. Purif. Technol.* 2018, **190**, 60-67.

[21] D. Wang, Z. Liu, L. Xu, C. Li, D. Zhao, G. Ge, Z. Wang, J. Lin, *Dalton Trans.* 2019, **48**, 278-284.

[22] Y. Wang, W. Fan, X. Wang, Y. Han, L. Zhang, D. Liu, F. Dai. D. Sun, *Inorg. Chem. Front.* 2018, **5**, 2408-2412.

[23] Y. Chen, Z. Qiao, D. Lv, H. Wu, R. Shi, Q. Xia, H. Wang, J. Zhou, Z. Li, *Ind. Eng. Chem. Res.* 2017, **56**, 4488-4495.

[24] W. Fan, X. Liu, X. Wang, Y. Li, C. Xing, Y. Wang, W. Guo, L. Zhang, D. Sun, *Inorg. Chem. Front.* 2018, **5**, 2445-2449.

[25] Y.-Z. Li, G.-D. Wang, R. Krishna, Q. Yin, D. Zhao, J. Qi, Y. Sui, L. Hou, *Chem. Eng. J.* 2023, **466**, 143056.

[26] X. H. Han, K. Gong, X. Huang, J. W. Yang, X. Feng, J. Xie, B. Wang, *Angew. Chem. Int. Ed.* 2022, **61**, e202202912.

[27] L. Zhang, L.-N. Ma, G.-D. Wang, L. Hou, Z. Zhu, Y.-Y. Wang, *J. Mater. Chem. A* 2023, **11**, 2343-2348.

[28] P. Guo, M. Chang, T. Yan, Y. Li, D. Liu, *Chin. J Chem. Eng.* 2022, **42**, 10-16.

[29] Y. Zhang, L. Yang, L. Wang, X. Cui, H. Xing, *J. Mater. Chem. A* 2019, **7**, 27560-27566.

[30] Z. Zeng, W. Wang, X. Xiong, N. Zhu, Y. Xiong, Z. Wei, J. J. Jiang, *Inorg. Chem.* 2021, **60**, 8456-8460.

[31] L. Wang, W. Sun, S. Duttwyler, Y. Zhang, *J Solid State Chem.* 2021, **299,** 122167.

[32] Y. Yuan, H. Wu, Y. Xu, D. Lv, S. Tu, Y. Wu, Z. Li, Q. Xia, *Chem. Eng. J.* 2020, **395**, 125057.